

Precise sub-pixel size measurement with linear interpolation

AIJUN YIN¹, ZHENGYI YANG^{2*}, GUANGQIAN LONG¹

¹The State Key Laboratory of Mechanical Transmission, Chongqing 400044, China

²School of Software Engineering, Chongqing University, Chongqing 401331, China

*Corresponding author: zyyang@cqu.edu.cn

High precision automated size measurements are required during industrial and scientific applications. The principle of sub-pixel measuring is based on an intensity interpolation algorithm. Combined with the characteristics of light, a system with high precision, short measuring time and low cost was developed. The proposed system is then applied to the measurement of 5 cm objects and compared with traditional measuring techniques. The experiment demonstrates that the measuring accuracy can reach up to 0.012 μm , and that the measurement size of the system is practical and prompt. In addition, it is able to meet the requirement for industrial applications in a variety of settings with stable performance and high precision.

Keywords: geometry size measurement, linear image sensor, linear interpolation algorithm.

1. Introduction

With the rapid improvement of industrial manufacturing and processing technology, geometry size measurement techniques have already played an important role in modern industry. There is an urgent need to develop advanced detection methods that are capable of high speed and precision in order to keep pace with the increasing demand in industry standards. Geometry size measurement techniques can be classified as either contact or non-contact methods, according to measuring force. Contact measurement methods mainly use a probe to obtain the target object parameters through direct contact of the surface. These include a caliper, micrometer, plug gauge, ring gauge, *etc.* Contact measurement methods are susceptible to equipment precision and human factors, and are restricted by the number of tools and users availability during analysis. The contact measurement method is limited on precision and efficiency. In order to improve the precision of measurement, more complicated and expensive equipment can be used, for instance a three-dimensional measuring machine, or an optical image-measuring machine. The non-contact measuring method is based on photoelectric and electromagnetic technology and can obtain surface parameters of the target object

without contacting the surface. This gives non-contact measuring higher precision, faster response and is damage free as compared to contact measurement methods.

Vision measurement technology is a non-contact measurement method that provides full field measurement, high precision and a high degree of automation. It has been widely studied and applied to industrial applications, and image-processing technology. Theoretical methods and detection instrumentation technology for visual inspection have been highly researched in developed countries. United States and Japan currently have high standards that have been widely applied to industry, *i.e.*, IO Industries (Canada), Siemens (Germany), OGP (United States), Keyenc (Japan), *etc.*

According to the visual inspection theory, linear interpolation of the pixel position measurement system has been studied [1]. SLADEK *et al.* studied the visual measurement of deflection and accuracy assessment [2]. LAMY and BASSET studied the wheel camber angle and visual inspection radius of a tire [3]. SAMPSON *et al.* studied the dual-view computer-vision system for volume and image texture analysis in multiple apple slices during drying [4]. GIROLAMI *et al.* studied the quantitative assessment of meat color using a computer vision system [5]. Furthermore, visual measurement sensor technologies have been widely studied [6–8].

In order to improve the detection accuracy, the edge detection and extraction method based on sub-pixel was studied thoroughly. The sub-pixel mechanisms are commonly used in the fitting method, moment method and specific sub-pixel detection methods that are currently under development. The general accuracy of the sub-pixel algorithm is 0.1–0.5 pixels, and some can be up to 0.01 pixels under ideal circumstances. LI QINGLI *et al.* utilized a quadratic polynomial in order to construct the interpolation function that verifies the location of the edge via an edge graph. Its precision can reach 1/85.3 pixel [9]. CUI JIWEN and TAN JIUBIN proposed an algorithm based on the Zernike moment sub-pixel location using error compensation, and its accuracy can reach 0.05 pixels for linear location [10].

Generally, visual measurements require a complex optical system, which is costly. It is difficult to achieve generalization, automation, intelligence and portable detection [11]. In order to solve the problems related to visual measurements, this paper provides a visual measurement system based on linear array light intensity with a higher theoretical accuracy of 0.012 μm . It is small, fast, accurate and instant in terms of performance [12].

The paper is organized as follows. Section 2 discusses the principles of optical measurement and design of the image acquisition system; Section 3 introduces the sub-pixel accurate measurements method based on light intensity interpolation; Section 4 presents the experimental set-up and results. The conclusions are given in Section 5.

2. Principle of measurement

The principle of measurement is shown in Fig. 1. An imaging system is placed on a height-adjustable bracket, and the measuring range increases with an increase in height, although its accuracy reduces with an increase in height. The measured object

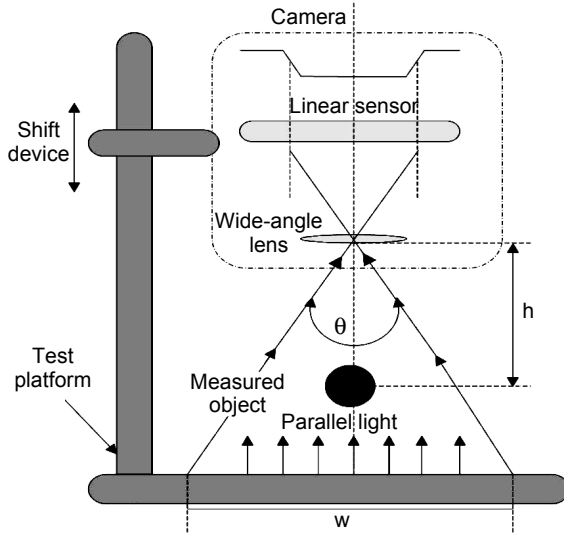


Fig. 1. The system measuring principle.

is placed between the light source and the imaging system, forming a curve of variable light intensity on the sensor when imaging. Through the analysis and calculation of the light intensity curve, the trim size of the measured object can be received. For the purpose of minimizing the outside interference and improving the measurement accuracy, a single light source is employed for measurement [13].

The optical measurement module is composed of a light source, photoelectric sensor and lens (Fig. 1). The system adopts a high brightness LED parallel light source, and a high aperture, wide-angle lens (81°). Farthest distance of detection can be up to 1 m. The high-performance CMOS linear array image sensor ELIS-1024 from Panvision Company with 1024 pixels is used, and it has a size of 7.8 μm. This sensor is capable of high integration and has a high signal-to-noise ratio. It is widely used in portable visual processing equipment.

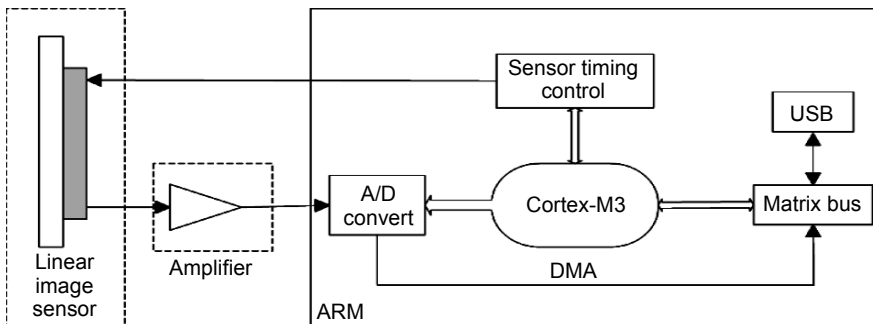


Fig. 2. Hardware structure of the acquisition system.

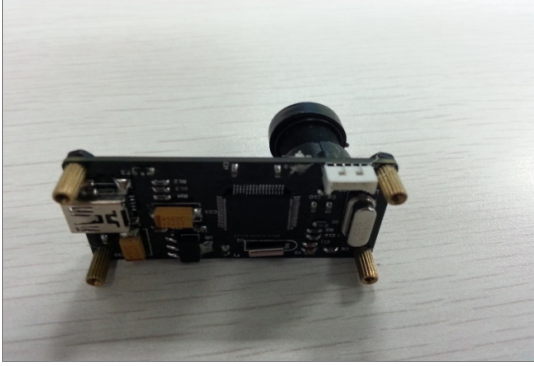


Fig. 3. Acquisition module.

The signal acquisition module is composed of a sensor driver circuit, data acquisition controller, transmission interface, *etc.* (Fig. 2). The system has a light intensity A/D conversion accuracy of 12 bit, the highest sample frequency is 700 kHz and is capable of high-speed USB data transmission (Fig. 3).

3. Sub-pixel accurate measurements based on light intensity interpolation

There are mainly three linear array image sensor data processing algorithms conventionally used: binarization processing, floating threshold method, and exposure adaptive algorithm [7]. The method of sub-pixel accurate measurement based on light intensity interpolation has been proposed, and its basic process involves the calibration of the threshold using a standard length and a sub-pixel measurement based on the threshold segmentation.

3.1. Calibration of the sub-pixel threshold

Initially, the system utilizes standard values for calibration, determining the measurement threshold. This paper employs the linear interpolation algorithm of adaptive threshold.

According to the measurement principle in Fig. 1, when the height between the lens and the object is h , the lens angle is θ , the measurement range (span) is:

$$S = 2h \tan(0.5\theta) \quad (1)$$

The ideal length of the image is $W = kM = 7.8M$ (where M is the number of pixels of the CMOS sensor, and pixel width is $k = 7.8 \mu\text{m}$). Therefore, the corresponding actual length μ of the unit image length (μm) is

$$\mu = \frac{S}{W} = \frac{2h \tan(0.5\theta)}{kM} \quad (2)$$

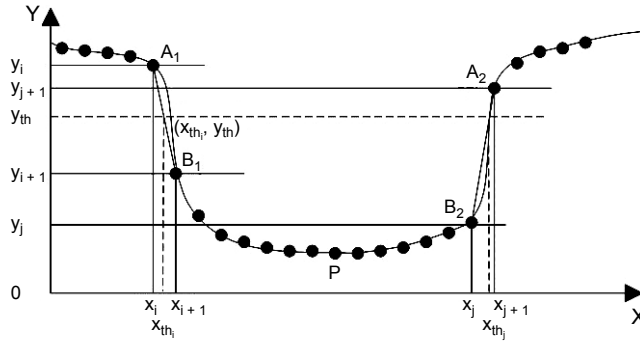


Fig. 4. Schematic of the interpolation algorithm.

The corresponding actual length β of each pixel k is

$$\beta = \mu k = \frac{S}{M} = \frac{2h \tan(0.5 \theta)}{M} \quad (3)$$

The threshold determination process is shown in Fig. 4, where X is the location of the pixel, Y is the light intensity obtained by the CMOS sensor. Given the standard length l , the theoretical number of pixels can be obtained by formula (3):

$$N = [l/\beta] \quad (4)$$

where $[]$ is to fetch an integer.

The minimum intensity P of the image as a starting point increases gradually until the number of pixels reaches N (Fig. 4). Setting the two edge points $B_1(x_{i+1}, y_{i+1})$, $B_2(x_j, y_j)$ and adjacent points $A_1(x_i, y_i)$, $A_2(x_{j+1}, y_{j+1})$ of B_1 and B_2 , gives the length of A_1B_1 , A_2B_2 , as pixel width, is $7.8 \mu\text{m}$. Given that the corresponding light intensity (theoretical threshold) of the standard parts edge is $y = y_{th}$, the corresponding image abscissae are x_{thj} , x_{thi} , respectively. Therefore the corresponding image length of a standard piece with the width of l is as follows:

$$L = x_{thj} - x_{thi} = kN + l_1 + l_2 \quad (5)$$

where $l_1 = x_{i+1} - x_{thj}$, $l_2 = x_{thi} - x_j$ (in μm). By formula (2), we can obtain

$$l = \mu L \quad (6)$$

With the geometric relationship in Fig. 4, and using linear interpolation, we can obtain

$$\begin{cases} \frac{l_1}{y_{th} - y_{i+1}} = \frac{x_{i+1} - x_i}{y_i - y_{i+1}} \\ \frac{l_2}{y_{th} - y_j} = \frac{x_{j+1} - x_j}{y_{j+1} - y_j} \end{cases} \quad (7)$$

where $x_{i+1} - x_i = x_{j+1} - x_j = 7.8$, and formulas (3), (5), (6), and (7) can be solved as

$$y_{\text{th}} = \frac{y_i y_j + y_{i+1} y_{j+1} - 2y_{i+1} y_j}{y_i - y_j + y_{j+1} - y_{i+1}} + \frac{(l - N\beta)(y_i - y_{i+1})(y_{j+1} - y_j)}{\beta(y_i - y_j + y_{j+1} - y_{i+1})} \quad (8)$$

Here, y_{th} is the threshold of the system measurement. The system installation error and the temperature excursion of the sensor will affect the threshold in actual application due to the intensity of the light source. Therefore, the threshold needs to be recalibrated [14].

3.2. Sub-pixel measurement

First, the measurement is segmented in order to obtain the light intensity curve, with the threshold as y_{th} . The number of pixels of the light intensity is lower than threshold as N' , therefore the length of the image is:

$$l_{\text{thr}} = N'k \quad (9)$$

According to Fig. 4, given that threshold edge points are $B'_1(x'_{i+1}, y'_{i+1})$ and $B'_2(x'_j, y'_j)$, respectively, the two adjacent points are $A'_1(x'_i, y'_i)$ and $A'_2(x'_{j+1}, y'_{j+1})$, respectively, and the length of the sub-pixel image can be obtained by formula (7) as:

$$l_{\text{sub}} = l'_1 + l'_2 = k \left(\frac{y_{\text{th}} - y'_{i+1}}{y'_i - y'_{i+1}} + \frac{y_{\text{th}} - y'_j}{y'_{j+1} - y'_j} \right) \quad (10)$$

The corresponding image length of the measured image is $L' = l_{\text{thr}} + l_{\text{sub}}$. The measuring length is:

$$l = \mu L' = \mu(l_{\text{thr}} + l_{\text{sub}}) \quad (11)$$

The size of the target object can be solved by combining Eqs. (3), (9), (10) and (11) to obtain

$$l = \beta \left(\frac{y_{\text{th}} - y'_{i+1}}{y'_i - y'_{i+1}} + \frac{y_{\text{th}} - y'_j}{y'_{j+1} - y'_j} \right) + N'\beta \quad (12)$$

3.3. Analysis of precision

Here, a sub-pixel thinning measurement algorithm is achieved by utilizing the interpolation to the light intensity transformation of the adjacent pixels (Fig. 4). Given that the maximum light intensity is P , the light intensity resolution $\Delta = P/2^n$ (where n is the resolution of A/D conversion of the light intensity). For Eq. (7), the length of image is $l_1 = k(y_{\text{th}} - y_{i+1})/(y_i - y_{i+1})$.

Under the ideal conditions $y_i - y_{i+1} = P$, $y_{th} - y_{i+1} = \Delta$, then:

$$l_1 = \frac{x_{i+1} - x_i}{2^n} = \frac{k}{2^n} \quad (13)$$

which is the measurement accuracy of the system sub-pixel image. By Eq. (2), the ideal accuracy of the system is

$$\sigma = l_1 \mu = \frac{2h \tan(0.5\theta)}{2^n M} \quad (14)$$

Equation (14) shows that the smaller h and θ are, the higher the A/D conversion resolution n of the light intensity and picture element M of sensors. The higher the accuracy of picture element, the lower the accuracy [14, 15].

3.4. Error analysis of the system

The formula (3), (8), (12) derivations are:

$$\Delta\beta = \frac{2 \left[\tan(0.5\theta)\Delta h + 0.5h \cot(0.5\theta)\Delta\theta \right]}{M} \quad (15)$$

$$\Delta y_{th} = \left(\frac{\Delta l}{\beta} - \frac{l\Delta\beta}{\beta^2} \right) \frac{(y_i - y_{i+1})(y_{j+1} - y_j)}{y_i - y_j + y_{j+1} - y_{i+1}} \quad (16)$$

$$\Delta l = \left(\frac{y_{th} - y'_{i+1}}{y'_i - y'_{i+1}} + \frac{y_{th} - y'_j}{y'_{j+1} - y'_j} \right) \Delta\beta + N' \Delta\beta + \left(\frac{1}{y'_i - y'_{i+1}} + \frac{1}{y'_{j+1} - y'_j} \right) \beta \Delta y_{th} \quad (17)$$

where $\left(\frac{y_{th} - y'_{i+1}}{y'_i - y'_{i+1}} + \frac{y_{th} - y'_j}{y'_{j+1} - y'_j} \right)$ and $\left(\frac{1}{y'_i - y'_{i+1}} + \frac{1}{y'_{j+1} - y'_j} \right) \beta$ are the transfer functions of $\Delta\beta$ and Δy_{th} to Δl .

4. Experimental design and analysis

4.1. The measurement system and results

The high precision sub-pixel measurement system developed is shown in Fig. 5. The distance between the lens and the measured object is $h = 2.930$ cm, the measurement range (span) obtained by Eq. (1) is $S = 5$ cm, pixel width $k = 7.8$ μm , the A/D conversion resolution of light intensity is $n = 12$, system sub-pixel localization accuracy is 0.0019 pixel

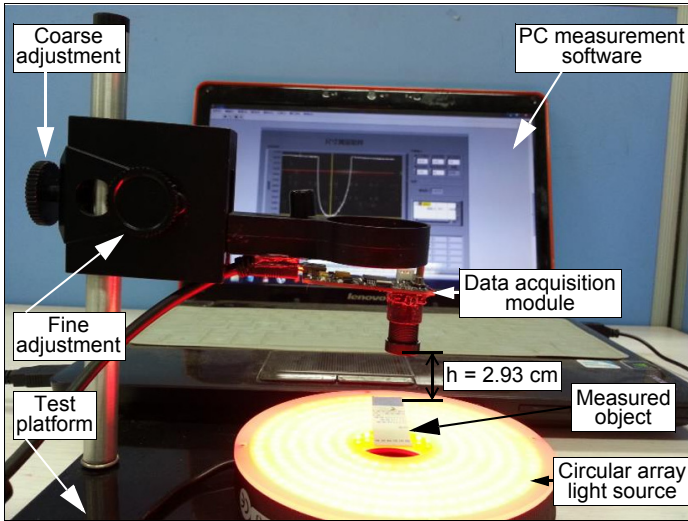


Fig. 5. Measurement system.

T a b l e 1. Experimental data compared to micrometer measurement data.

Data using micrometer [mm]	Data using proposed system [mm]	Uncertainty
6.699	6.699023	0.000267
10.000	10.000057	0.000216
11.706	11.705817	0.000460
14.020	14.023656	0.000271
15.000	15.000086	0.000175
15.878	15.877837	0.000360
18.768	18.768551	0.000330
20.000	20.000015	0.000324
22.000	22.000200	0.000515

as calculated by Eq. (13), the pixel number of the sensor is $M = 1024$, and the lens angle $\theta = 81^\circ$. The ideal measurement accuracy is $0.012 \mu\text{m}$ as calculated by Eq. (14).

Table 1 shows a set of measured data under the conditions described above as compared to a micrometer. The measuring precision of the micrometer is 0.01 mm . This 3rd digit is estimated. Data using the proposed system are calculated with Eq. (12). The uncertainty values are calculated using the following equation:

$$u_{(A)} = f(n)s_{(\bar{x})} = f(n)\sqrt{\frac{\sum_{i=1}^n (x_i - \bar{x})^2}{n(n-1)}} \quad (18)$$

where n is the measurement number, x_i is the measured data, \bar{x} is the average number of x , $f(n)$ is associated with the confidence factor (generally taken as 1 on the line), and s is the standard deviation of the average.

By comparison with the micrometer, the experimental data illustrates that the test results of the proposed system are accurate and efficient at measuring.

The errors of the measured values fluctuated within the range, which indicates the stability and reliability of the system as compared to using a micrometer.

4.2. Error factors of the system

Systematic and random errors inevitably exist within the measurement system, and are mainly caused by the following factors.

The influence of light source system – In the measurement system, dark spots formed on the CMOS sensor via the object to be tested and covered the parallel light source. The edge interpolation algorithm then calculates the covered pixel amount in order to achieve the dimension value. Therefore the collimation and stability of the linear array light source affect the measurement results directly. In the ideal model, a projected linear array light source should be parallel. But in practice, because of the influence of the divergence of light source, a stable parallel light source cannot be received, causing an error within the measurements.

The influence of CMOS image sensor – Here, the selected sensor had 1024 pixels. According to Eq. (2), the resolution of the system is inversely proportional to the number of pixels. In other words, the greater the number of pixels, the higher the precision. In addition, in terms of the structure of the CMOS image sensor, and through analyzing the light sensitive characteristics, fill factor and compensation pixels, it was found that the distribution of the pixels is not homogeneous. In consequence, the edge error is produced during measurements, and the output voltage of the sensor changed slightly with the variation in temperature.

The influence of testing platform – The height between the lens and the measured object cannot be adjusted to the theoretical value, resulting in transformation of β and the generation of the system error. When the measured object is completely perpendicular to the sensor, the obtained value is the actual value, while if the measured object and the sensor are into a certain angle, the size would be measured with deviations leading errors.

5. Conclusion

Visual measuring technique with the characteristics of non-contact, high precision and higher automation has been widely researched and applied. This paper provides a measurement system based on the linear array CMOS image sensor. The basic principle of measurement is introduced, and the linear array image data acquisition module, op-

tical imaging system of measurement and construction of measurement principle are developed. The sub-pixel adaptive threshold selection principle (calibration) based on light intensity linear interpolation is studied thoroughly. Sub-pixel accurate measurement has been realized, and precision of the measuring system and the influencing factor of errors are analyzed. By comparing with a high-precision size measuring system, it shows that the proposed system can measure the geometric dimension of an object quickly and accurately. The system is low cost, small in dimensions and is simple to use. It provides a new measuring method for high-precision detection in automatic production.

According to Eq. (14), the system measurement accuracy depends on the measuring height h , lens angle θ , light intensity A/D conversion digit n and the number of sensor pixels. This system adopts a sensor with 1024 pixels and A/D conversion resolution of 12 bit. Both the number of pixels and A/D conversion digit impact the accuracy. Selecting a sensor with more pixels and an A/D chip with higher performance in order to improve precision would greatly improve the system. The size measurement system that takes into account the influence of light source, temperature excursion of sensor testing platform, *etc.*, would further improve the system and allow for higher precision measurement.

Acknowledgements – The work is supported by the National Natural Science Foundation of China under Grant No. 61271167 and No. 51105396 and the Fundamental Research Funds for the Central Universities under Grant No. CDJZR13115501 and No. 106112013CDJZR090004.

References

- [1] FISCHER J., PRIBULA O., *Precise subpixel position measurement with linear interpolation of CMOS sensor image data*, The 6 IEEE International Conference on Intelligent Data Acquisition and Advanced Computing system: Technology and Applications, September 15–17, 2011, pp. 500–504.
- [2] SŁADEK J., OSTROWSKA K., KOHUT P., HOLAK K., GAŠKA A., UHL T., *Development of a vision based deflection measurement system and its accuracy assessment*, *Measurement* **46**(3), 2013, pp. 1237–1249.
- [3] LAMY C., BASSET M., *A vision-based approach to wheel camber angle and tyre loaded radius measurement*, *Sensors and Actuators A: Physical* **161**(1–2), 2010, pp. 134–142.
- [4] SAMPSON D.J., YOUNG KI CHANG, VASANTHA RUPASINGHE H.P., QAMAR UZ ZAMAN, *A dual-view computer-vision system for volume and image texture analysis in multiple apple slices drying*, *Journal of Food Engineering* **127**(4), 2014, pp. 49–57.
- [5] GIROLAMI A., NAPOLITANO F., FARAONE D., BRAGHERI A., *Measurement of meat color using a computer vision system*, *Meat Science* **93**(1), 2013, pp. 111–118.
- [6] QUINE B.M., TARASYUK V., MEBRAHTU H., HORNSEY R., *Determining star-image location: a new sub-pixel interpolation technique to process image centroids*, *Computer Physics Communications* **177**(9), 2007, pp. 700–706.
- [7] KARIMIRAD F., CHAUHAN S., SHIRINZADEH B., *Vision-based force measurement using neural networks for biological cell microinjection*, *Journal of Biomechanics* **47**(5), 2014, pp. 1157–1163.
- [8] JONG-WOONG PARK, JONG-JAE LEE, HYUNG-JO JUNG, HYUN MYUNG, *Vision-based displacement measurement method for high-rise building structures using partitioning approach*, *NDT & E International* **43**(7), 2010, pp. 642–647.

- [9] LI QINGLI, *et al.*, *A improved subpixel edge detecting algorithm based on polynomial interpolation*, Journal of Jilin University (Engineering and Technology Edition) **25**(3), 2003, pp. 280–283, (in Chinese).
- [10] CUI JIWEN, TAN JIUBIN, *Algorithm for edge subpixel location based on Zernike moment*, Optical Technique **31**(5), 2005, pp. 779–785.
- [11] IZADPANAHI S., DEMIREL H., *Motion based video super resolution using edge directed interpolation and complex wavelet transform*, Signal Processing **93**(7), 2013, pp. 2076–2086.
- [12] *STM32 Reference Manual*.
- [13] MALMBERGA F., LINDBLAD J., SLADOJE N., NYSTRÖM I., *A graph-based framework for sub-pixel image segmentation*, Theoretical Computer Science **412**(15), 2011, pp. 1338–1349.
- [14] SHAN Y., BOON G.W., *Sub-pixel location of edges with non-uniform blurring: a finite closed-form approach*, Image and Vision Computing **18**(13), 2000, pp. 1015–1023.
- [15] RAMDANI S., BOUCHARA F., DJEMAL K., *Probability distribution of sub-pixel edge position*, Signal Processing **84**(3), 2004, pp. 445–452.

*Received July 9, 2014
in revised December 2, 2014*